BORON CHEMISTRY AND QUANTIFICATION IN LOW ENERGY BORON IMPLANTED SILICON BY X-RAY PHOTOELECTRON SPECTROSCOPY

Jeffrey R. Shallenberger[1]
Evans Analytical Group, 104 Windsor Center Dr. #104, E. Windsor NJ 08520

Steven Walther
Varian Semiconductor Equipment Associates, 35 Dory Rd., Gloucester MA 01930

As the dopant concentration in the outer 5 nm of low energy implants reaches percent levels, x-ray photoelectron spectroscopy (XPS) offers several unique attributes that make it a valuable metrology tool. The combination of surface sensitivity, straightforward quantification and chemical state specificity are found in no other analytical tool. In this paper, we examine a number of as-implanted and annealed BF_2 and $^{11}B^+$ samples by XPS with a focus on the near-surface boron chemical environment. Boron is observed in at least three different chemical states (B_2O_3, boron-interstitial-clusters (BIC) and 4-coordinated with silicon) in selected samples. The dose of boron in the oxide layer (atoms/cm^2) and the average near-surface concentration (in atoms/cm^3) can be directly measured and are demonstrated to provide important information in the outer few nm of these complex materials.

INTRODUCTION

Boron is the most widely used *p*-type dopant in silicon devices. The preferred method of doping is ion implantation. This process introduces significant lattice damage and the implanted boron must be electrically activated by a thermal annealing step. Unfortunately, annealing leads to both transient enhanced diffusion (TED) of boron aided by the presence of Si interstitials- creating deeper than desired junctions - as well as the formation of insoluble boron-containing clusters. These materials have been extensively modeled (1-4) and experimentally probed by secondary ion mass spectrometry (2,4-7), transmission electron microscopy (5), electron energy loss spectroscopy (8) and channeling nuclear reaction analysis.(9,10) These studies have involved doping methods that create large numbers of interstitial defects (ion implantation) as well as approaches where the interstitial concentration was low (e.g., solid phase epitaxial regrowth, MBE, CVD). It has been found that boron-containing clusters form in the presence of high concentrations of interstitial silicon atoms. These boron-interstitial-clusters, abbreviated BIC or B_nI_m (where n is the number of boron atoms and m is the number of Si interstitials) are electrically inactive even after thermal annealing. In this paper we examine the near-surface boron chemical environment on a series of low energy $^{11}B^+$ and BF_2^+ implants with x-ray photoelectron spectroscopy (XPS) to quantitatively determine the types of boron present after implantation and spike annealing.

Historically, XPS (also known as ESCA) has not been utilized to characterize ion implanted semiconductors because of the limited sampling depth (1-10 nm) and relatively poor sensitivity (detection limits of 10^{19}-10^{20} atoms/cm^3). However, with the advent of low energy, high dose implants a significant fraction of the dose now resides within the reach of XPS. Fortunately XPS offers several unique attributes that can help characterize these complex materials. Principally, it is one of the few surface techniques that can determine local chemical bonding. Perturbations in the core electron binding energies can often be correlated – usually with the aid of reference materials - to nearest neighbor chemical environment. Quantification of photoelectron spectra is relatively straightforward. Databases of photoelectron cross sections and instrumental parameters are available. The resulting Relative Sensitivity Factors (RSFs) are,

[1] Electronic mail: jshallenberger@eaglabs.com

to a first approximation, independent of the local chemistry. Thus, XPS offers the ability to not only detect dopants in the near-surface but also determine the amount of each chemical state present.

Several groups have studied boron implanted silicon or related materials by XPS in the past. Shallenberger *et al.* examined 1-10 keV $^{11}B^+$, BF_2^+ and As^+ implants with an emphasis on determining oxide layer thickness and quantifying dopant incorporation within the oxide as a function of implant energy and anneal.(11) They found B doses within the oxide layer approaching 20% of the total dose on as-implanted wafers. Yang *et al.* examined the oxidation of amorphous and crystalline boron and a Si:B (25% B) alloy and found boron *1s* peaks corresponding to three-coordinated B in Si (186.6 eV) and four-coordinated B in Si (187.7 eV) as well as sub-oxides of boron at higher binding energy.(12) Mizushima *et al.* observed four distinct boron 1s peaks under different anneal conditions using both low pressure chemical vapor deposition (8) and ion implantation (13). They interpreted these boron peaks as divalent, trivalent, quadrivalent and B_{12} clusters, with divalent and trivalent favored at low temperatures and the quadrivalent and clusters favored at T>600°C. Based on the reported peak position, the phrase "quadrivalent" by Mizushima *et al.* likely does not mean B^{4+}, rather it refers to boron with four bonds to silicon and is thus, the same as four-coordinated boron reported by Yang *et al*. Ohmori *et al.* used simulated XPS spectra to conclude that B_6 (at 188.1 eV) was the preferred cluster in as-implanted high dose boron.(14)

In this work we will present the results from a series of $^{11}B^+$ and BF_2^+ implanted silicon samples by XPS and correlate changes in the boron 1s peak positions with changes in the local boron chemical environment. A new term, the average near-surface boron concentration, is introduced and used to compare the XPS data with SIMS data.

EXPERIMENTAL

X-ray photoelectron spectroscopy measurements were performed on a Physical Electronics model 5701 LSci instrument equipped with monochromatic x-ray source (hv=1486.7 eV) and concentric hemispherical analyzer. Samples were analyzed at takeoff angles of 30° and 65° to probe the surface and sub-surface, respectively. No charge neutralization was utilized during data acquisition. Charge correction was done by fixing the adsorbed hydrocarbon peak in the carbon 1s spectra to 285.0 eV. This correction resulted in the Si $2p_{3/2}$ component of the substrate silicon being present at 98.7 ±0.1 eV. XPS quantification was done by applying instrumental relative sensitivity factors (RSFs) to the integrated peak areas of Si 2p, C 1s, B 1s, O 1s and F 1s spectra.

The Si 2p and B 1s spectra were curve fit to separate the overlapping spectral components. Four sets of doublets were used to fit the Si 2p spectra. These doublets are attributed to the spin orbital split Si° (98.7±0.1 eV), SiO_2 (102.8±0.3 eV), SiO_x (101.1±0.2 eV) and a small elemental silicon peak inserted to account for the natural asymmetry of the Si° component.(15) The boron fits are discussed below.

The finite sampling depth of XPS presents difficulties when comparing dopant concentration with other analytical techniques because elemental concentrations are typically normalized to 100% and include signal from the adsorbed organic, native oxide and any impurities present. In this paper we introduce a value designed to permit a more direct comparison with SIMS data in the near-surface region immediately beneath the oxide. This value is the average near-surface boron concentration, $B_{avg}(\theta)$ defined as,

$$B_{avg}(q) = \frac{\left(\frac{I_{B1s}(q)}{RSF_{B1s}}\right)}{\left(\frac{I_{B1s}(q)}{RSF_{B1s}} + \frac{I_{Si2p}(q)}{RSF_{Si2p}}\right)} * N_{Si°} \qquad \text{Eqn. (1)}$$

The terms $I_{B\,1s}(\theta)$ and $I_{Si\,2p}(\theta)$ refer to the experimentally determined intensities of reduced boron and elemental silicon. The RSF_{Si2p} and RSF_{B1s} terms are the relative sensitivity factors for Si and B; N_{Si} is the atom density of silicon (assumed to be 5.0×10^{22} atoms/cm^3). The intensities of these species are strongly dependent on sampling depth-which in turn varies with the sine of the takeoff angle, θ. Thus different B_{avg} values will be measured at different takeoff angles permitting a qualitative determination of boron depth distribution. This approach suffers from one known systematic error: the resulting concentration *assumes* a constant B:Si ratio within the 2-5 nm sampling depth of XPS. Thus the average

near-surface concentration will be only used as a precise measure of dopant concentration over a somewhat ill-defined sampling depth.

The tested samples, 300 mm Si (100) with a native oxide, were implanted at a 0° implant angle with either $^{11}B^+$ or BF_2^+ using a Varian VIISta HCP single wafer, high current implanter with the noted dose and energy values. Sample annealing was performed with a Mattson 3000 Plus RTP tool using a 1050°C spike anneal and an ambient of nitrogen with 300 ppm oxygen, unless otherwise noted.

RESULTS

A. Boron chemical environment

Figure 1 shows a low energy resolution survey spectrum along with high energy resolution Si 2p and B 1s spectra (insets) acquired from a Si (100) wafer implanted with 1 keV BF_2^+ ions to a dose of 3 x 10^{15} atoms/cm^2. The boron 1s spectrum overlaps with a broad Si 2s plasmon peak, but boron is clearly detected as a peak centered at ~186.5 eV. A weak B_2O_3 peak is detected at 192.5 eV. Curve fitting (Figure 2) reveals a third boron peak present at 187.6 eV on the as implanted BF_2 wafer (Fig. 2a). After spike annealing at 1050°C, the 186.5 eV peak disappears. Similar behavior was observed higher energy (Fig. 2c and 2d), at lower dose (not shown), and even on a 0.2 keV $^{11}B^+$ implant (not shown). For the sample matrix chosen in this study, 50-80% of boron detected on the as-implanted samples was present at 186.5 ±0.1 eV with the remaining boron present at 187.6±0.1 eV. After spike annealing, 100% of the boron detected was present at 187.6±0.1 eV.

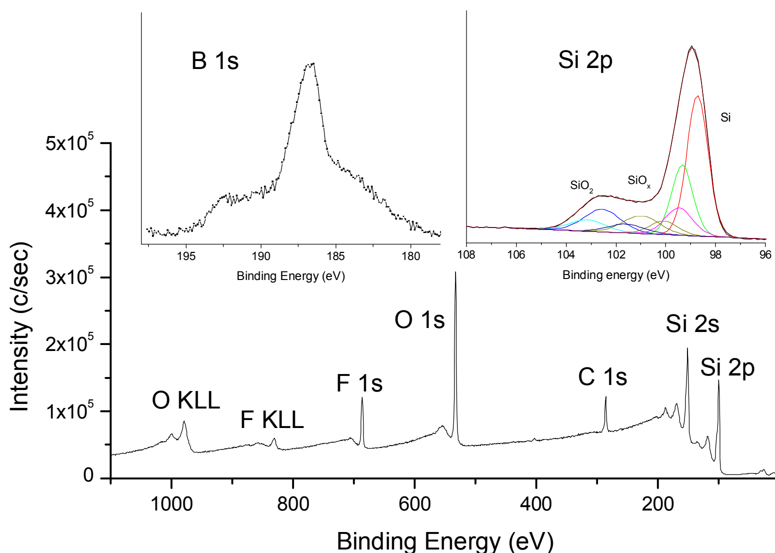

Figure 1. Low resolution survey spectrum from ion implanted silicon wafer. Insets show boron 1s (top, left) and silicon 2p (top, right) spectra. The Si 2p spectrum has been curve fit into oxide, substrate and sub-oxide components.

The 186.5 eV peak is 1.6 eV lower in binding energy than the reported position for elemental boron but in excellent agreement with reports of metal borides such as MgB_2.(16) This strongly suggests that this peak contains B and Si as opposed to a pure boron phase. More clues about the identity of this peak are available in work published on samples with similar implant and anneal conditions. Cristiano *et al.* (5) observed small interstitial dislocation loops on {100} planes 2.5 nm below the surface on as-implanted and low temperature (<650°C) annealed 500 eV $^{11}B^+$ 1 x 10^{15} implants via TEM. Monte Carlo simulations concluded roughly 90% of boron in as-implanted Si was due to boron-interstitial clusters with the balance present as substitutional.(3) Using channeling NRA, Romano *et al.* concluded a small, two-atom B-B complex was present after implantation and that these complexes were transformed into larger clusters during annealing.(10) Based on the similar implant conditions and concentrations we conclude that the 186.5 eV peak observed on all as-implanted samples is due to boron-interstitial-clusters (BIC).

After a 1010°C anneal on 1 keV $^{11}B^+$ 1 x 10^{15} implant, Monte Carlo simulations by Aboy *et al.* indicated ~80% of the boron was substitutional.(2) The BICs observed by TEM disappeared after 1050°C spike annealing.(5) Romano *et al.* (10) made a similar conclusion based on channeling NRA results from a 50 keV $^{11}B^+$ 2 x 10^{15} atoms/cm^2 sample annealed at T>950°C. Thus, we conclude that the photoemission peak observed at 187.6 eV on the spike annealed $^{11}B^+$ and BF_2^+ samples is due primarily to substitutional boron. The peak at the identical energy on the as-implanted samples- which are known to be amorphous within the XPS sampling depth- may be better described as “four-coordinated boron” (i.e., B surrounded

by four Si atoms, but not necessarily on a Si lattice site).(12) The proximity of elemental boron from this study (188.1 eV) as well as other reports of B_{12} (13) or B_6 (14) cluster positions leaves open the possibility that some fraction of the boron detected at 187.6 eV is the result of one or more of these species.(1)

B. Quantification of near-surface average boron

Table I summarizes the wealth of information available from XPS. Spike annealing results in 0.1-0.2 nm growth in the surface oxide. The dose of boron in the SiO_2 is highest on the 0.2 keV $^{11}B^+$ 10^{15} implant, despite the fact that an equivalent energy (1 keV) BF_2^+ implant with three times the dose was analyzed. The B_{avg} data for the two reduced species is presented at the different takeoff angles to provide qualitative information about the depth distribution. The most common variable used to describe sampling depth in XPS is inelastic mean free path, λ. The effective sampling depth varies as λsin(θ), where θ is the takeoff angle. Using λ_{Si2p} of 3.4 nm as representative of the signals detected, the estimated sampling depths at 30° and 65° are 1.7 and 3.0 nm, respectively. In all cases the variable takeoff angle data indicate a decreasing boron concentration in the sub-surface, i.e., B_{avg} (30°) > B_{avg} (65°). The BF_2 implants show a larger B_{avg} (30) / B_{avg} (65) after annealing compared with the as-implanted BF_2 samples suggesting a steeper fall in the boron profile after spike annealing. This finding is confirmed by SIMS (Fig. 3) for the as-implanted (black) and annealed

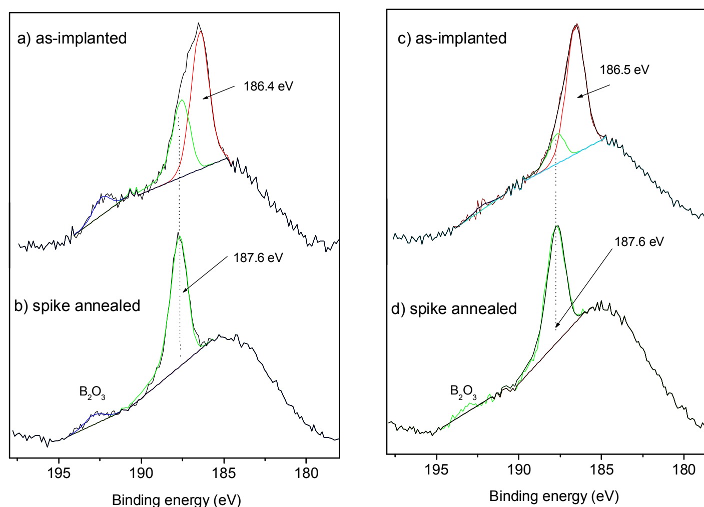

Figure 2. High resolution boron 1s spectra from BF_2^+ implanted at (a) 1 keV, 3 x 10^{15} atoms/cm^2 as-implanted, (b) 1 keV, 3 x 10^{15} atoms/cm^2 spike annealed, (c) 3 keV 3 x 10^{15} atoms/cm^2 as-implanted and (d) 3 keV 3 x 10^{15} atoms/cm^2 spike annealed. The peak present at 186.5 eV disappears after spike annealing.

Table 1. Summary of information obtained by angle resolved XPS measurements

Implant	Condition	t_{ox} nm	B^{3+} in SiO_2 atoms/cm^2	Angle	BIC atoms/cm^3	B-(Si_4) atoms/cm^3	Total B_{avg} atoms/cm^3
BF_2^+ 1 keV, 1 x 10^{15}	as-implanted	1.08	7.3 x 10^{13}	30°	1.3 x 10^{21}	4.6 x 10^{20}	1.7 x 10^{21}
				65°	1.0 x 10^{21}	3.0 x 10^{20}	1.4 x 10^{21}
	annealed	1.31	3.8 x 10^{13}	30°	-	1.1x x 10^{21}	1.1 x 10^{21}
				65°	-	6.9 x 10^{20}	6.9 x 10^{20}
BF_2^+ 1 keV, 3 x 10^{15}	as-implanted	1.19	6.6 x 10^{13}	30°	1.9 x 10^{21}	2.1 x 10^{21}	4.0 x 10^{21}
				65°	1.6 x 10^{21}	1.6 x 10^{21}	3.2 x 10^{21}
	annealed	1.35	7.1 x 10^{13}	30°	-	4.3 x 10^{21}	4.3 x 10^{21}
				65°	-	2.6 x 10^{21}	2.6 x 10^{21}
BF_2^+ 3 keV, 3 x 10^{15}	as-implanted	0.79	4.2 x 10^{13}	30°	1.8 x 10^{21}	5.6 x 10^{20}	2.3 x 10^{21}
				65°	1.6 x 10^{21}	6.0 x 10^{20}	2.2 x 10^{21}
	annealed	0.94	8.0 x 10^{13}	30°	-	2.7 x 10^{21}	2.7 x 10^{21}
				65°	-	2.1 x 10^{21}	2.1 x 10^{21}
$^{11}B^+$ 0.2 keV, 1 x 10^{15}	as-implanted	1.05	1.3 x 10^{14}	30°	1.3 x 10^{21}	5.5 x 10^{20}	1.9 x 10^{21}
				65°	1.1 x 10^{21}	2.9 x 10^{20}	1.3 x 10^{21}
	annealed	1.14	9.3 x 10^{13}	30°	-	1.9 x 10^{21}	1.9 x 10^{21}
				65°	-	1.2 x 10^{21}	1.2 x 10^{21}

(red) 1 keV, BF_2^+ 3 x 10^{15} atoms/cm^2 implant. After annealing boron diffuses into the silicon and, simultaneously, forms a more abrupt near-surface distribution.(17)

Another notable effect was observed on the equivalent kinetic energy $^{11}B^+$ (0.2 keV) and BF_2^+ (1 keV) samples. The as-implanted wafers were virtually identical with the exception of a higher F concentration in the near-surface region of the BF_2 implant and roughly twice the boron concentration in the SiO_2 layer. After spike annealing, however, the average boron near surface concentration was ~70% higher on the $^{11}B^+$ implanted wafer compared with the BF_2^+ implanted annealed.

There is good quantitative agreement with the near-surface SIMS data. B_{avg}(65°) for the as-implanted 1 keV 3 x 10^{15} BF_2^+ implant is 3.2 x 10^{21} atoms/cm^3; the spike annealed sample which drops more quickly has B_{avg}(65°) of 2.6 x 10^{21} atoms/cm^3. SIMS measures an average B concentration below the SiO_2 interface to a depth of ~8 nm of 3 x 10^{21} atoms/cm^3 on both samples.

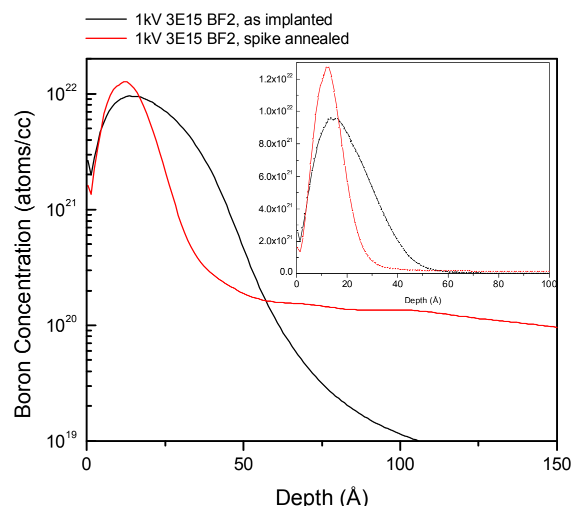

Figure 3. PCOR-SIMS^{SM} depth profiles of as-implanted (black) and annealed (red) 3 x 10^{15}, 1 keV BF_2^+ implants into Si (100). The inset - plotted on a linear concentration scale- demonstrates that the overwhelming majority of the dopant resides within the 5-10 nm analysis depth of XPS.

Other trends detected by XPS include a strong effect of dose on near-surface concentration; higher dose leads to higher B_{avg} although not 3X the near-surface concentration. Lower implant energy at equivalent dose and species leads to higher B_{avg} because more of the dose is within the top ~3 nm.

In summary, it was demonstrated that XPS can be used to detect and quantify boron-interstitial-clusters (BIC) in as-implanted $^{11}B^+$ and BF_2^+ samples. The characteristic boron 1s peak due to BIC is present at a binding energy of 186.5 ±0.1 eV. The average BIC near-surface concentration ranged from 10^{21} to 2 x 10^{21} atoms/cm^3 and was a function of dose, although apparently not a function of energy within the XPS sampling depth. The fraction of BIC on as-implanted samples ranged from 50-80% of the total boron, in good agreement with previously published TEM, channeling NRA and Monte Carlo simulation studies. The remaining boron on the as-implanted wafers was due to boron four-coordinated to silicon. Spike annealing converted the BIC to substitutional or possibly a pure boron (B_{12}, B_6) species present at 187.6±0.1 eV. The relative distribution and concentration of boron in the near-surface agreed well with SIMS measurements. Finally, the boron dose present within the ~1 nm SiO_2 layer was directly measured and found also to be a function of implant and anneal conditions. Up to 14% of the intended dose was deposited within the oxide.

ACKNOWLEDGEMENTS

The authors would like to thank Mr. John Marino and Dr. Ming Hong Yang of Evans Analytical Group for providing the SIMS depth profiles and to Drs. Charles Magee and Wesley Nieveen for thoughtful discussions.

REFERENCES

[1] S. Solmi, E.Landi, F.Baruffaldi, J. Appl. Phys. 68 3250 (1990).
[2] N.E.B. Cowern,M.J.J. Theunissen, F.Roozeboom, J.G.M. van Berkum, Appl. Phys. Lett. 75 181 (1999).
[3] M. Aboy, L.Pelaz, L.A. Marques, P. Lopez, J.Barbolla, R. Duffy, J. Appl. Phys. 97 103520 (2005).
[4] G.Mannino, N.E.B. Cowern, F. Roozeboom, J.G.M. van Berkum App. Phys. Lett. 76 855 (2000).

[5] F. Cristiano, X. Hebras, N.Chaerkashin, A. Claverie, W. Lerch and S. Paul, App. Phys. Lett. 83 5407 (2003).
[6] D. De Salvador, E.Napolitani, G.Bisognin, A. Carnera, E.Bruno, S. Mirabella, G.Impellizzeri and F.Priolo, App. Phys. Lett. 87 221902 (2005).
[7] S. Walther, L. Godet, T. Buyuklimanli, J.Weeman, J.Vac.Sci.Technol. B24 489 (2006).
[8] I. Mizushima, Y.Mitani, M.Koike, M.Yoshiki, M.Tomita and S. Kambayashi, Jpn. J. Appl. Phys. 37 1171 (1998).
[9] A.M.Piro, L.Romano, S.Mirabella, M.G. Grimaldi, App. Phys. Lett., 86 081906 (2005).
[10] L.Romano, A.M.Piro, S.Mirabella, M.G. Grimaldi, E. Rimini, App. Phys. Lett. 87 201905 (2005).
[11] J.R. Shallenberger, D.A. Cole, D.F. Downey, S.Falk, Z.Zhao, 1998 Ion Implantation Technology Proceedings, International Conference on 566 (1999).
[12] G.-R. Yang, Y.-P. Zhao, M. Abburi, S. Dabral and B.Y. Tong, J.Vac. Sci. Technol. A 15(2) 279 (1997).
[13] I. Mizushima, A. Murakoshi, K. Suguro, N. Aoki and J. Yamauchi", Mater. Chem. Phys. 54 54 (1998).
[14] K. Ohmori, N.Esashi, M.Takao, D.Sato, Y.Hayafuji, App. Phys. Lett. 87 112101 (2005).
[15] J.R. Shallenberger, D.A.Cole, S.W. Novak, J.Vac.Sci.Technol A 17(4) 1086 (1999).
[16] R.P. Vasquez, C.U. Jung, M-S. Park, H-J. Kim, J.Y. Kim, S-I.Lee, Phys. Rev. B 64 052510 (2001).
[17] H. Graoui, M.A. Foad, Mat. Sci. Eng. B 124-125 188 (2005).